

Weakness of whole muscles in mice deficient in Cu, Zn superoxide dismutase is not explained by defects at the level of the contractile apparatus

Lisa M. Larkin · Michael C. Hanes ·
Erdan Kayupov · Dennis R. Clafin ·
John A. Faulkner · Susan V. Brooks

Received: 21 October 2011 / Accepted: 21 May 2012 / Published online: 14 June 2012
© American Aging Association 2012

Abstract Mice deficient in Cu,Zn superoxide dismutase (*Sod1*^{-/-} mice) demonstrate elevated oxidative stress associated with rapid age-related declines in muscle mass and force. The decline in mass for muscles of *Sod1*^{-/-} mice is explained by a loss of muscle fibers, but the mechanism underlying the weakness is not clear. We hypothesized that the reduced maximum isometric force (F_o) normalized by cross-sectional area (specific F_o) for whole muscles of *Sod1*^{-/-} compared with wild-type (WT) mice is due to decreased specific F_o of individual fibers. Force generation was measured for permeabilized fibers from muscles of *Sod1*^{-/-} and WT mice at 8 and 20 months of age. WT mice were also studied at 28 months to determine whether any deficits observed for fibers from *Sod1*^{-/-} mice were similar to those observed in old WT mice. No effects of genotype were observed

for F_o or specific F_o at either 8 or 20 months, and no age-associated decrease in specific F_o was observed for fibers from *Sod1*^{-/-} mice, whereas specific F_o for fibers of WT mice decreased by 20 % by 28 months. Oxidative stress has also been associated with decreased maximum velocity of shortening (V_{max}), and we found a 10 % lower V_{max} for fibers from *Sod1*^{-/-} compared with WT mice at 20 months. We conclude that the low specific F_o of muscles of *Sod1*^{-/-} mice is not explained by damage to contractile proteins. Moreover, the properties of fibers of *Sod1*^{-/-} mice do not recapitulate those observed with aging in WT animals.

Keywords Contractility · Oxidative stress · Permeabilized fiber · Skeletal muscle · Specific force

Introduction

Aging is accompanied by a decline in skeletal muscle mass and a deficit in muscle function often referred to as sarcopenia. The mechanisms underlying the age-related declines in mass and function are not known, but alterations in the production and handling of reactive oxygen species (ROS) generated by the muscle have been proposed as contributing factors (Fulle et al. 2004). Contraction-induced production of ROS has been shown to cause oxidative stress in skeletal muscle (Ji 2008) despite the presence in muscle of extensive and interacting ROS buffering systems (Ji et al. 2009). Aging is associated with an increase in the

L. M. Larkin · M. C. Hanes · J. A. Faulkner · S. V. Brooks
Departments of Molecular and Integrative Physiology,
University of Michigan,
Ann Arbor, MI 48109-2200, USA

L. M. Larkin · E. Kayupov · D. R. Clafin · J. A. Faulkner ·
S. V. Brooks (✉)
Biomedical Engineering, University of Michigan,
Ann Arbor, MI 48109, USA
e-mail: svbrooks@umich.edu

D. R. Clafin
Surgery, Section of Plastic Surgery, University of Michigan,
Ann Arbor, MI 48109, USA

activities of antioxidant enzymes in skeletal muscle (Jackson 2009; Ji 2007; Muller et al. 2006), but whether the increase is sufficient to protect against ROS-induced muscle damage in senescent animals is not clear (Jackson & McArdle 2011). The hypothesis that ROS contribute to the age-associated decline in muscle function proposes that either an age-associated increase in ROS production in skeletal muscle or a decrease in the effectiveness of ROS defense mechanisms (Ji 2007) leads to ROS damage in muscle that accumulates with age and decreases mass and force production.

The effects observed experimentally of ROS on contractile function are highly complex and vary greatly in both a time- and dose-dependent manner (Reid et al. 1993). The variability reflects, at least in part, an apparent requirement of low levels of ROS in skeletal muscle for normal force generation (Reid 2001). Oxidative stress is chronically and dramatically elevated in all tissues of mice deficient in Cu,Zn superoxide dismutase (*Sod1*^{-/-} mice) compared to wild type *Sod1*^{+/+} mice (WT), including skeletal muscle (Muller et al. 2006). Accompanying the high levels of oxidative stress, muscles of *Sod1*^{-/-} mice display an accelerated age-associated loss of mass and force (Jang et al. 2010; Larkin et al. 2011; Muller et al. 2006). The maximum isometric force (F_o) normalized by total muscle fiber cross-sectional area (CSA) (specific F_o) for gastrocnemius (GTN) muscles of 8-month-old *Sod1*^{-/-} mice is not different from that of 20-month-old WT mice, and specific F_o is also similar for GTN muscles of 20-month-old *Sod1*^{-/-} mice and 28-month-old WT mice (Larkin et al. 2011). This accelerated decline in muscle function for *Sod1*^{-/-} mice with properties similar to age-associated sarcopenia suggests that the *Sod1*^{-/-} mouse may represent a model for studying the role of oxidative stress in the development of muscle weakness with aging.

High oxidative stress decreases force generation in part through direct effects of oxidative modifications of contractile or regulatory proteins (Andrade et al. 1998; Plant et al. 2000). The 30–40 % deficit in specific F_o observed for whole GTN muscles of 8- and 20-month-old *Sod1*^{-/-} mice (Larkin et al. 2011) indicate that either individual fibers within these muscles also show 30–40 % deficits in force generation or most fibers generate normal forces while many fibers generate essentially no force and thus contribute

to CSA, but not to force. Some combination of fibers with a wide range of contractile deficits may also exist. In order to distinguish between these possibilities, contractile properties of single permeabilized muscle fibers from medial gastrocnemius (MGN) muscles of 8- and 20-month-old *Sod1*^{-/-} and WT mice were compared. Fibers were also obtained from 28-month-old WT mice to determine whether any deficits observed for fibers from *Sod1*^{-/-} mice were similar to those observed in old WT mice. In addition to the effects of oxidative stress-induced disruption of actin–myosin interactions to reduce active force generation (Lowe et al. 2001), treatment with ROS has been shown to decrease velocity of shortening (Prochniewicz et al. 2008). Thus, the hypothesis was tested that single permeabilized fibers from MGN muscles of *Sod1*^{-/-} mice exhibit lower values for specific F_o , lower shortening velocities, and lower power output than fibers of WT mice at 8 and 20 months of age and that the deficits are similar to those seen in fibers from muscles of WT mice at 28 months.

Methods

Animals and animal care

Male *Sod1*^{-/-} and *Sod1*^{+/+} (WT) mice were generously provided by Dr. Holly Van Remmen at the University of Texas Health Science Center at San Antonio. To allow comparisons with our previous studies of the function of whole GTN muscles (Larkin et al. 2011), *Sod1*^{-/-} and WT mice were studied at 8 and 20 months of age. WT mice were also studied at 28 months, an age when muscle atrophy and weakness, defined as reduced specific F_o , have been previously observed for hind-limb muscles of mice (Brooks & Faulkner 1988; Larkin et al. 2011). Animals were acquired at ~6, ~18, or ~26 months (WT mice only) of age and maintained under barrier conditions in a temperature-controlled environment and were fed a commercial mouse chow (Teklad diet LM485) ad libitum until they reached the appropriate ages for testing. All mice were housed in specific pathogen-free facilities both prior to and after their arrival at the University of Michigan. All experimental procedures were approved by the University Committee for the Use and Care of Animals at the University of Michigan and were in accordance with the

Guide for Care and Use of Laboratory Animals (Public Health Service, 19965, NIH Pub. No. 85-23).

Acquisition and storage of permeabilized muscle fibers

Mice were anesthetized with intraperitoneal injections of 2 % avertin (tribromoethanol, 250 mg/kg). Supplemental doses were administered as required to maintain a depth of anesthesia sufficient to prevent response to tactile stimuli. The medial gastrocnemius muscle was isolated from surrounding muscle and connective tissue. The muscle was placed immediately into cold skinning solution and 8–12 bundles of fibers approximately 4–6 mm in length and 0.5 mm in diameter were dissected from each muscle. Following dissection, bundles were immersed for 30 min in skinning solution to which the nonionic detergent Brij 58 had been added (0.5 % w/v). Fiber bundles were then placed in storage solution and maintained for 16–24 h at 4 °C followed by storage at –20 °C for up to 2.5 months before use.

Measurement of isometric contractile properties

On the day of an experiment, fiber bundles were removed from storage solution and placed in relaxing solution on ice. Single fibers were pulled manually from the bundle with fine forceps and transferred to an experimental chamber containing relaxing solution maintained at 15 °C. One end of the fiber was secured to a force transducer (Aurora Scientific, Inc., Model 403A) using two ties of 10-0 monofilament nylon suture. The other end of the fiber was attached in a similar manner to the lever arm of a servomotor (Aurora Scientific, Inc., Model 322 C). The length of the fiber was adjusted to obtain a sarcomere length of 2.5–2.6 μm , determined by projecting a laser diffraction pattern produced by the fiber onto a calibrated target screen. Fiber length (L_f) was then measured by first aligning the innermost tie at one end of the fiber with the crosshairs of a microscope eyepiece graticule, then translating the entire apparatus with respect to the microscope using a micrometer drive with digital read-out until the innermost tie at the other end of the fiber was aligned with the crosshairs. Fiber CSA was estimated at L_f using fiber width and depth measurements from high-magnification digital images of both top and side views of the fiber (Panchangam et al. 2006). Side views were obtained using a prism embedded in the side of the bath. Five width–depth measurement

pairs were obtained at $\sim 100\text{-}\mu\text{m}$ intervals along the midsection of the fiber. Fiber cross-sectional areas were calculated for each width–depth pair assuming an elliptical cross-section, and overall CSA was estimated by averaging the five individual areas.

Relaxed single fibers were activated by first immersing them in a chamber containing a low- $[\text{Ca}^{2+}]$ preactivating solution for 3 min followed by immersion in a chamber containing a high- $[\text{Ca}^{2+}]$ activating solution (pCa ~ 4.5) to elicit maximum isometric force (F_o). The preactivating solution was weakly buffered for Ca^{2+} , resulting in very rapid activation and force development upon introduction of the activating solution (Moiescu & Thieleczek 1978). The solution-changing system (Aurora Scientific, Inc., Model 802A) consisted of six separate glass-bottom chambers machined into a moveable, temperature-controlled stainless-steel plate. Movement of the plate with respect to the fiber was achieved by remote-control of two stepper motors, one to lower and raise the chamber array, and the other to translate the plate to a new chamber position. Specific F_o was calculated by dividing F_o by fiber CSA.

Solutions

The *skinning solution* was composed of the following (in millimolar): potassium propionate, 125; imidazole, 20; ethyleneglycol-bis (B-aminoethyl ether) tetraacetic acid (EGTA), 5; MgCl_2 , 2; ATP, 2; dithiothreitol, 1; and leupeptin, 0.1. The composition of the storage solution was identical to that of skinning solution with the exception that glycerol was substituted for 50 % of the water volume. The *relaxing solution* (pCa ≈ 9.0) was composed of the following (in millimolar): HEPES, 90; Mg (total), 10.3; Mg^{2+} , 1.0; EGTA, 50; ATP, 8.0; CrP, 10.0; NaN_3 , 1.0; Na (total), 36; K (total), 125. The *preactivating solution* was as follows (in millimolar): HEPES, 90; Mg (total), 8.50; Mg^{2+} , 1.0; EGTA, 0.10; 1,6-diaminohexane-N,N,N',N'-tetraacetic acid (HDTA), 50; ATP, 8.0; CrP, 10.0; NaN_3 , 1.0; Na (total), 36; K (total), 125. The *activating solution* (pCa ≈ 4.5) was as follows (in millimolar): HEPES, 90; Mg (total), 8.12; Mg^{2+} , 1.0; EGTA, 50; Ca (total), 50; ATP, 8.0; CrP, 10.0; NaN_3 , 1.0; Na (total), 36; K (total), 125. The pH of all solutions was adjusted to 7.1 at 15 °C. Potassium propionate and HDTA were obtained from TCI America, and all other compounds are obtained from Sigma Chemical.

Measures of force–velocity characteristics

Force–velocity characteristics were evaluated as previously described (Claflin et al. 2011). Briefly, forces were measured during a series of constant-velocity ramp shortening movements initiated from a length 10 % longer than L_f and applied to maximally activated fibers. The force associated with a given shortening speed was measured at the time that the fiber had shortened by 10 % of L_f , and consequently, its length was passing through L_f . Force was measured relative to the baseline revealed by a post-ramp step and was normalized by the maximum isometric force measured just prior to application of the shortening movement. This procedure resulted in 8–12 data points to which a rectangular hyperbola was fitted. Maximum velocity of shortening (V_{\max}) was determined as the point at which the fitted hyperbola intersected the velocity axis (force=0) and was normalized by fiber length (L_f /per second). Force–power curves were generated from the parameters of the fitted curve, and maximum power (P_{\max}) was measured as the peak of the force–power curve. Finally, P_{\max} was divided by fiber volume ($L_f \times \text{CSA}$) to obtain normalized P_{\max} (nP_{\max} , watts·per liter).

Data acquisition and statistical analyses

Force responses and motor position were acquired at 5 k samples s^{-1} through a 16-bit A-D board (NI-6052-PCI, National Instruments) and displayed and stored on a personal computer using a custom-designed LabVIEW program (National Instruments). The position of the motor was updated at a rate of 10 ks^{-1} by the LabVIEW program via a D-A channel on the acquisition board. All data are reported as means \pm standard error of the mean. Two-factor analysis of variance (ANOVA) was used to determine the effect on fiber properties of genotype (*Sod1*^{-/-} vs. WT) and age for the 8- and 20-month groups. Data from 28-month-old WT mice were compared to all other groups by one way ANOVA or Kruskal–Wallis ANOVA on ranks in cases when the normality or equal variance test failed. When significance was detected, Tukey's (ANOVA) or Dunn's (ANOVA on ranks) post hoc comparison was used to assess the individual differences. In all cases, the level of significance was set a priori at $p=0.05$.

Results

Consistent with our previous report (Larkin et al. 2011) of no differences between GTN muscles of *Sod1*^{-/-} and WT mice for average single fiber CSAs determined from histological cross sections, CSAs of single permeabilized fibers from MGN muscles were also not different between genotypes in the present study (Fig. 1). Although the two-factor ANOVA indicated a significant age effect for single fiber CSAs, post-hoc analyses revealed that no differences between individual groups reached significance. Also consistent with our previous histological analyses (Larkin et al. 2011), CSA did not decrease significantly with age for single fibers from MGN muscles of WT mice, even at the advanced age of 28 months.

Analysis of isometric contractile properties of single fibers from MGN muscles indicated that there was a significant age-associated decline in F_o between 8 and 20 months for both genotypes (Fig. 2a), although, similar to the findings for CSA, no differences between individual groups reached significance. In addition, fibers from WT mice showed a continued progressive decline in force generation such that by 28 months, F_o was significantly lower than the value observed for

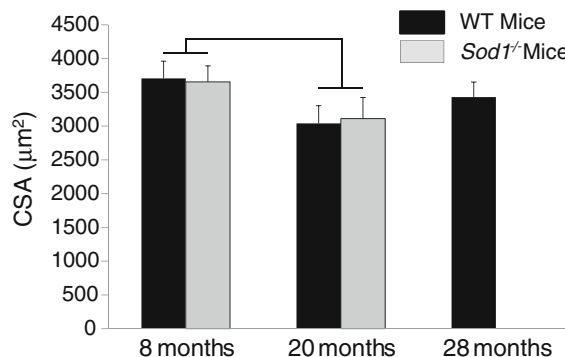


Fig. 1 Cross-sectional areas are shown for permeabilized fibers from medial gastrocnemius muscles of WT mice (black bars) and CuZnSOD-deficient (*Sod1*^{-/-}) mice (gray bars) of varying ages. Areas are expressed in square micrometers. Data are presented as means \pm one standard error of the mean. Sample sizes are $N=20$, 21, and 19 for WT mice at 8, 20, and 28 months, respectively; and $N=25$ and 20 for 8 and 20 months *Sod1*^{-/-} mice, respectively. Two-factor ANOVA showed a significant age effect between 8- and 20-month values, as indicated by the bracket; but post-hoc analysis revealed no individual differences

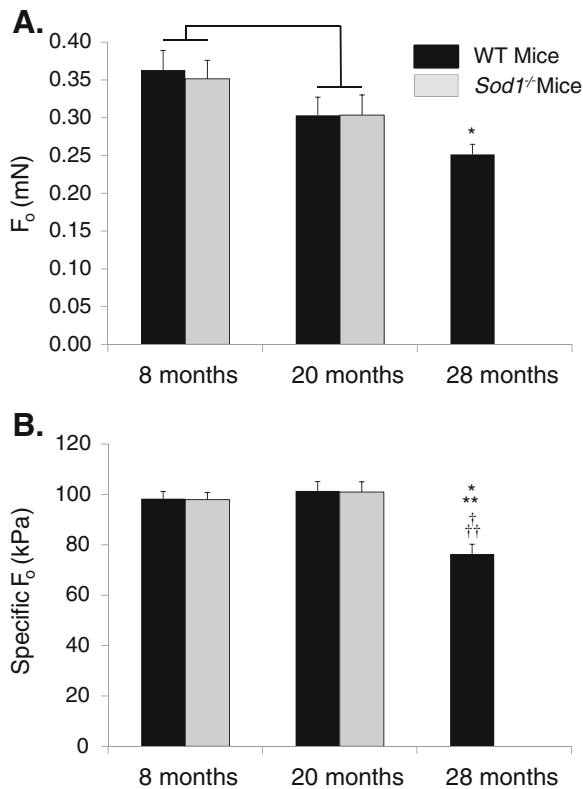


Fig. 2 **a** Maximum isometric force (F_o) and **b** F_o normalized by fiber cross-sectional area (specific F_o) are shown for permeabilized fibers from medial gastrocnemius muscles of WT mice (black bars) and CuZnSOD-deficient (*Sod1*^{-/-}) mice (gray bars) of varying ages. F_o is expressed in millinewtons and specific F_o is expressed in kilopascals. Data are presented as means \pm one standard error of the mean. Sample sizes are as indicated in Fig. 1. Two-factor ANOVA showed a significant age effect between 8- and 20-month values for F_o , as indicated by the bracket; but post-hoc analysis revealed no individual differences. No significant genotype or age effects were seen by two-factor ANOVA for specific F_o . Symbols indicate significant differences determined by one-way ANOVA. Single asterisk, different from WT mice at 8 months; double asterisks, different from WT mice at 20 months; dagger, different from *Sod1*^{-/-} mice at 8 months; double daggers, different from *Sod1*^{-/-} mice at 8 months

fibers of 8-month-old animals. Despite previous reports of lower force generation by whole GTN muscles of *Sod1*^{-/-} compared with WT mice at 8 and 20 months of age (Larkin et al. 2011), F_o for single permeabilized fibers from MGN muscles was not affected by genotype at either age. Also in contrast to the findings of dramatic weakness for whole GTN muscles of *Sod1*^{-/-} compared with WT mice at both 8 and 20 months (Larkin et al. 2011), specific F_o was not affected by genotype

(Fig. 2b). Although data from whole GTN muscles also showed increasing weakness with age for both *Sod1*^{-/-} and WT mice, there was no decline in the specific F_o of single permeabilized fibers between 8 and 20 months for either genotype. In contrast, the value for specific F_o was significantly lower for single fibers from MGN muscles of 28-month-old WT mice compared with the values for every other group of fibers studied (Fig. 2b).

Contrary to our hypothesis, V_{max} was not different between MGN fibers from *Sod1*^{-/-} and WT mice at 8 months. Despite the similarity in velocity of shortening at 8 months, V_{max} decreased between 8 and 20 months for fibers from *Sod1*^{-/-} mice while fibers from WT mice showed no change, resulting in a V_{max} that was significantly slower for MGN fibers from *Sod1*^{-/-} compared with WT mice at 20 months (Fig. 3). Moreover, a decreasing trend for WT mice between 20 and 28 months of age resulted in values of V_{max} for fibers from MGN muscles of 20-month-old *Sod1*^{-/-} mice and 28-month-old WT mice that were not different.

The average maximum power values for each group are shown in Fig. 4. Consistent with the lack of an effect of genotype on either F_o or V_{max} at 8 months, P_{max} values were also not different for MGN fibers of *Sod1*^{-/-} and WT mice at that age. Similarly, despite the difference in V_{max} between fibers of *Sod1*^{-/-} and WT mice at 20 months, the lower

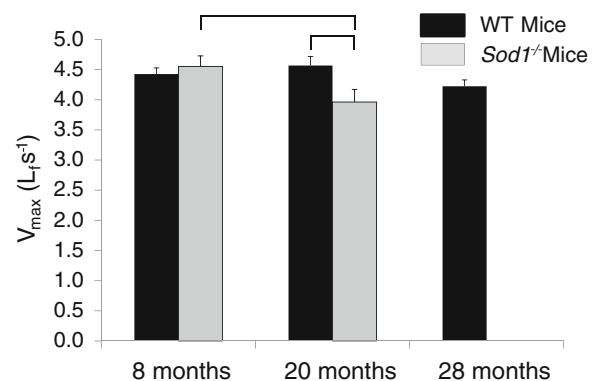


Fig. 3 Maximum velocity of shortening (V_{max}) is shown for permeabilized fibers from medial gastrocnemius muscles of WT mice (black bars) and CuZnSOD-deficient (*Sod1*^{-/-}) mice (gray bars) of varying ages. V_{max} is expressed in fiber lengths per second. Data are presented as means \pm one standard error of the mean. Sample sizes are as indicated in Fig. 1. Two-factor ANOVA showed a significant age \times genotype interaction, post-hoc analysis revealed individual differences as indicated by the brackets

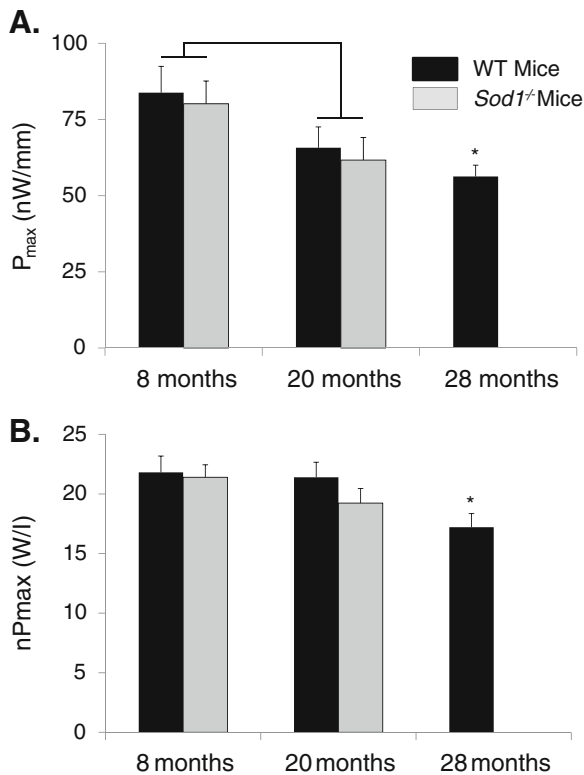


Fig. 4 **a** Maximum power (P_{\max}) and **b** P_{\max} normalized by fiber volume (nP_{\max}) are shown for permeabilized fibers from medial gastrocnemius muscles of WT mice (black bars) and CuZnSOD-deficient (*Sod1*^{-/-}) mice (gray bars) of varying ages. P_{\max} is expressed in nanowatts per fiber length and nP_{\max} is expressed in watts per liter. Data are presented as means \pm one standard error of the mean. Sample sizes are as indicated in Fig. 1. Two-factor ANOVA showed a significant effect between 8- and 20-month values for P_{\max} , as indicated by the bracket, but post-hoc analysis revealed no individual differences. No significant genotype or age effects were seen by two-factor ANOVA for nP_{\max} . Symbols indicate significant differences determined by one-way ANOVA. Asterisk, different from WT mice at 8 months

velocity for fibers of *Sod1*^{-/-} mice was not sufficient to decrease P_{\max} compared with the value for WT fibers. The age-associated declines in F_o produced similar age-associated effects on P_{\max} for fibers of *Sod1*^{-/-} mice between 8 and 20 months and for WT mice between 8 and 28 months. For fibers of *Sod1*^{-/-} mice, normalizing power by fiber volume eliminated the age effects on nP_{\max} , whereas fibers from MGN muscles of 28-month-old WT mice showed a 20 % deficit in nP_{\max} due primarily to the decreased specific force-generating capacity of fibers in this group. Although nP_{\max} decreased between 8 and 28 months for

fibers of WT mice, nP_{\max} for fibers of 28-month-old WT mice was not different from the value for *Sod1*^{-/-} mice of either other age group.

Discussion

In the present study, we hypothesized that the decrease in specific F_o previously reported by our group for whole muscles of *Sod1*^{-/-} mice (Jang et al. 2010; Larkin et al. 2011) would be explained by a decrease in the specific F_o of individual muscle fibers. Contrary to our hypothesis, no differences were observed in the maximum force-generating capacity of single permeabilized fibers from *Sod1*^{-/-} and WT mice at either 8 or 20 months of age. These data indicate that, when the contractile apparatus of fibers from *Sod1*^{-/-} mice is exposed to our high-[Ca²⁺] activating solution, there is no impairment in force. In order to gain a more complete assessment of the effects of chronic oxidative stress on contractile function, fibers were evaluated not only for maximum force generation under isometric conditions (F_o) but also at two additional points on the force–velocity relationship. V_{\max} provides an estimate of the maximum shortening velocities of fibers and represents a measure of function under unloaded conditions where the rate of myosin crossbridge detachment from actin dominates the response (Woledge et al. 1985), and normalized peak power (nP_{\max}) occurs at intermediate loads on the force–velocity relationship offering perhaps the most comprehensive index of overall contractile function (Podolin & Ford 1986). Evaluation of fiber contractility across the entire range of forces and velocities provided a full appraisal of the alterations in intrinsic function caused by chronic oxidative stress. The only difference between fibers from *Sod1*^{-/-} compared with WT mice was an ~10 % decline in V_{\max} at 20 months, a finding consistent with modest reductions in shortening velocity previously reported for skeletal muscle fibers of mice treated with physiological concentrations of peroxides (Andrade et al. 2001). While the lower V_{\max} observed for fibers from *Sod1*^{-/-} compared with WT mice suggests some deleterious effect of oxidative stress on the contractile proteins, this interpretation should be viewed with caution. As pointed out by Podolin and Ford (Podolin & Ford 1986), V_{\max} is an extrapolated value that is determined at a point on the force–velocity curve where velocity is highly sensitive to force. Thus, even small changes in any factor that

affects fiber response can be amplified to cause larger apparent changes in V_{\max} .

Although our findings indicate that the contractile proteins within muscle fibers of *Sod1*^{-/-} mice do not suffer irreversible damage as a result of chronic exposure to high oxidative stress, direct effects of oxidants on the myofibrillar apparatus that influence force generation have been reported (Andrade et al. 1998; Plant et al. 2001). Oxidative modifications of contractile proteins may disrupt actin – myosin interactions such that the number of myosin crossbridges strongly bound to actin is reduced, thereby reducing force-generating capacity of individual muscle fibers (Lowe et al. 2001), but the actual effects of ROS on contractile function are complex and dependent on the specific oxidizing agent as well as the levels and duration of treatment. For example, in isolated intact single fiber preparations, acute administration of H₂O₂ was reported to increase force production, whereas prolonged exposure to H₂O₂ decreased force-generating capacity (Andrade et al. 1998; Plant et al. 2001). Studies of skinned single fibers report effects of exposure to ROS that range from force enhancement (Darnley et al. 2001), to reductions in force (Callahan et al. 2001; Darnley et al. 2001), to no effect (Callahan et al. 2001; Lamb & Posterino 2003). This variability in response may reflect at least in part the requirement in skeletal muscle of low levels of ROS for normal force production (Reid 2001; Supinski & Callahan 2007). Indeed, antioxidant-mediated depletion of ROS from nonfatigued skeletal muscle results in a depression of muscle force production (Coombes et al. 2001; Reid et al. 1993). The positive impact of ROS on muscle force production is reversed at higher ROS concentrations as force production decreases in both a time- and dose-dependent manner (Reid et al. 1993).

Although we found little evidence in the present study for oxidative stress-induced deficits in function at the level of the contractile apparatus, the permeabilized fiber approach involves removing the fibers from the native in vivo environment. Fibers are stored and tested in solutions of standard composition with respect to calcium, ATP, and presumably ROS levels, and oxidative modifications that may have existed in vivo may be reversed by prolonged exposure to these standard solutions (Andrade et al. 1998). For example, contractile deficits observed in vitro, for muscles that demonstrated elevated oxidative stress due to high levels of circulating tumor necrosis factor-alpha in

vivo, were partially reversed by acute antioxidant treatment of the muscle (Li et al. 2000). Thus, muscle fibers of *Sod1*^{-/-} mice may have possessed contractile deficits in vivo that were not observed when the fibers were ultimately tested in our system.

In addition to the profound weakness of skeletal muscle associated with high oxidative stress in *Sod1*^{-/-} mice, the observation of deficits in specific force for GTN muscles of WT mice at 20 months of age (Larkin et al. 2011) along with reports of elevated protein oxidation in the muscles of WT mice of the same age (Muller et al. 2006) supports the possibility of a direct effect of increased oxidative stress and damage with aging on force generation. Despite a 25 % deficit in specific force for whole GTN muscles of 20-month-old compared with 8-month-old WT mice (Larkin et al. 2011), specific F_0 was not different for single fibers from MGN muscles of 8- and 20-month-old WT mice. Thus, the weakness observed in 20-month-old WT mice at the whole muscle level is not due to the inability of the contractile proteins to generate force and may have the same mechanistic basis as the weakness of *Sod1*^{-/-} mice. In contrast to the lack of an effect of the CuZnSOD deficiency on single fiber force and power observed in the present study, fibers from 28-month-old WT mice displayed 20 % declines in specific F_0 and nP_{\max} compared with the values for younger WT mice as well as a trend for a decrease in V_{\max} . Age-related deficits in force generation have been reported previously for individual fibers from flexor digitorum brevis, extensor digitorum longus, and soleus muscles of mice (Gonzalez et al. 2000; Jimenez-Moreno et al. 2008; Lowe et al. 2001), but the mechanism is not completely clear. In addition, deficits with aging in V_{\max} and nP_{\max} have been reported previously for both slow type 1 and fast type 2 fibers of humans (Claflin et al. 2011; Larsson et al. 1997) and rats (Degens et al. 1998; Li & Larsson 1996), but again the mechanisms have not been established. Damage to myofibrillar proteins by increased levels of reactive oxygen and/or nitrogen species has previously been proposed to play a role in the age-related decline in skeletal muscle force generation (reviewed in (Thompson 2009)). While our finding in the present study that single fibers from muscles of old WT mice displayed specific force deficits indicate that the age-associated weakness observed at the whole muscle level for gastrocnemius muscles of 28-month-old WT mice (Larkin et al. 2011) is explained by decreased function at the level of the contractile apparatus,

this deficit explained only about half of the 40 % deficit observed at the whole muscle level (Larkin et al. 2011).

An inherent weakness of the single permeabilized fiber preparation for use in studies such as this that attempt to correlate single fiber to whole muscle function is the issue of sampling. The gastrocnemius muscles of mice contain on the order of 10,000 fibers (Burkholder et al. 1994). Thus, whether our experimental groups of ~20 fibers each can be considered representative may be questioned. Despite this weakness in approach, we can conclude that, at the very least, numerous fibers exist in the muscles of *Sod1*^{-/-} mice that show no decrement in the force-generating capacity of the contractile proteins as a result of chronic exposure to an environment of high oxidative stress (Muller et al. 2006).

In summary, this study indicates that the deficits in specific force generation observed for whole GTN muscles of 8- and 20-month-old *Sod1*^{-/-} mice and 20-month-old WT mice is not explained by irreversible oxidative damage to contractile proteins. We cannot, however, rule out the possibility that oxidative modifications of the myofibrillar apparatus may influence muscle fiber function in vivo, whereas storage and testing in our standardized solutions abrogate the effects. The decreased ability of CuZnSOD-deficient muscles of *Sod1*^{-/-} mice to dismutate superoxide anion is expected to increase the availability of superoxide (Vasilaki et al. 2010). Superoxide can react with nitric oxide-producing peroxynitrite, thereby increasing 3-nitrotyrosine levels (Sakellariou et al. 2011), and an effect of protein tyrosine nitration to impair skeletal muscle contractility has been demonstrated (Supinski et al. 1999), although the effect may be greater in slow than in fast muscle fibers (Dutka et al. 2011), such as were studied in the present experiments. Additional as yet unidentified mechanisms underlying the weakness of muscles of *Sod1*^{-/-} mice may also be at play in 20-month-old WT mice, in which whole muscle weakness was not accompanied by deficits in single fiber function. Finally, the *Sod1*^{-/-} mice do not appear to represent a good model of accelerated aging with respect to single fiber function. That is, the F_0 of single permeabilized fibers showed age-associated declines that were remarkably similar

for fibers from muscles of both *Sod1*^{-/-} and WT mice, and the decline for both genotypes was due primarily to declining CSA. The decline in F_0 observed for the truly old 28-month-old WT mice was due to reduced specific F_0 with no further decline in CSA. Thus, the properties of single fibers of *Sod1*^{-/-} mice do not appear to recapitulate those observed with aging in WT animals.

Acknowledgments Financial support was provided by the National Institute on Aging, grant AG-020591.

Reference

- Andrade FH, Reid MB, Allen DG, Westerblad H (1998) Effect of hydrogen peroxide and dithiothreitol on contractile function of single skeletal muscle fibres from the mouse. *J Physiol* 509:565–575
- Andrade FH, Reid MB, Westerblad H (2001) Contractile response of skeletal muscle to low peroxide concentrations: myofibrillar calcium sensitivity as a likely target for redox-modulation. *FASEB J* 15:309–311
- Brooks SV, Faulkner JA (1988) Contractile properties of skeletal muscles from young, adult and aged mice. *J Physiol* 404:71–82
- Burkholder TJ, Fingado B, Baron S, Lieber RL (1994) Relationship between muscle fiber types and sizes and muscle architectural properties in the mouse hindlimb. *J Morphol* 221:177–190
- Callahan LA, She ZW, Nosek TM (2001) Superoxide, hydroxyl radical, and hydrogen peroxide effects on single-diaphragm fiber contractile apparatus. *J Appl Physiol* 90:45–54
- Clafin DR, Larkin LM, Cederna PS, Horowitz JF, Alexander NB, Cole NM, Galecki AT, Chen S, Nyquist LV, Carlson BM, Faulkner JA, Ashton-Miller JA (2011) Effects of high- and low-velocity resistance training on the contractile properties of skeletal muscle fibers from young and older humans. *J Appl Physiol* 111:1021–1030
- Coombs JS, Powers SK, Rowell B, Hamilton KL, Dodd SL, Shanely RA, Sen CK, Packer L (2001) Effects of vitamin E and alpha-lipoic acid on skeletal muscle contractile properties. *J Appl Physiol* 90:1424–1430
- Darmley GM, Duke AM, Steele DS, MacFarlane NG (2001) Effects of reactive oxygen species on aspects of excitation-contraction coupling in chemically skinned rabbit diaphragm muscle fibres. *Exp Physiol* 86:161–168
- Degens H, Yu F, Li X, Larsson L (1998) Effects of age and gender on shortening velocity and myosin isoforms in single rat muscle fibres. *Acta Physiol Scand* 163:33–40
- Dutka TL, Mollica JP, Lamb GD (2011) Differential effects of peroxynitrite on contractile protein properties in fast- and slow-twitch skeletal muscle fibers of rat. *J Appl Physiol* 110:705–716
- Fulle S, Protasi F, Di TG, Pietrangelo T, Beltramin A, Boncompagni S, Vecchiet L, Fano G (2004) The

- contribution of reactive oxygen species to sarcopenia and muscle ageing. *Exp Gerontol* 39:17–24
- Gonzalez E, Messi ML, Delbono O (2000) The specific force of single intact extensor digitorum longus and soleus mouse muscle fibers declines with aging. *J Membr Biol* 178:175–183
- Jackson MJ (2009) Skeletal muscle aging: role of reactive oxygen species. *Crit Care Med* 37:S368–S371
- Jackson MJ, McArdle A (2011) Age-related changes in skeletal muscle reactive oxygen species generation and adaptive responses to reactive oxygen species. *J Physiol* 589:2139–2145
- Jang YC, Lustgarten MS, Liu Y, Muller FL, Bhattacharya A, Liang H, Salmon AB, Brooks SV, Larkin L, Hayworth CR, Richardson A, Van Remmen H (2010) Increased superoxide in vivo accelerates age-associated muscle atrophy through mitochondrial dysfunction and neuromuscular junction degeneration. *FASEB J* 24:1376–1390
- Ji LL (2007) Antioxidant signaling in skeletal muscle: a brief review. *Exp Gerontol* 42:582–593
- Ji LL (2008) Modulation of skeletal muscle antioxidant defense by exercise: role of redox signaling. *Free Radic Biol Med* 44:142–152
- Ji LL, Gomez-Cabrera MC, Vina J (2009) Role of free radicals and antioxidant signaling in skeletal muscle health and pathology. *Infect Disord Drug Targets* 9:428–444
- Jimenez-Moreno R, Wang ZM, Gerring RC, Delbono O (2008) Sarcoplasmic reticulum Ca²⁺ release declines in muscle fibers from aging mice. *Biophys J* 94:3178–3188
- Lamb GD, Posterino GS (2003) Effects of oxidation and reduction on contractile function in skeletal muscle fibres of the rat. *J Physiol* 546:149–163
- Larkin LM, Davis CS, Sims-Robinson C, Kostrominova TY, Van Remmen H, Richardson A, Feldman EL, Brooks SV (2011) Skeletal muscle weakness due to deficiency of CuZn superoxide dismutase is associated with loss of functional innervation. *Am J Physiol Regul Integr Comp Physiol* 301(5):R1400–7
- Larsson L, Li X, Frontera WR (1997) Effects of aging on shortening velocity and myosin isoform composition in single human skeletal muscle cells. *Am J Physiol Cell Physiol* 272:C638–C649
- Li X, Larsson L (1996) Maximum shortening velocity and myosin isoforms in single muscle fibers from young and old rats. *Am J Physiol Cell Physiol* 270:C352–C360
- Li X, Moody MR, Engel D, Walker S, Clubb FJ Jr, Sivasubramanian N, Mann DL, Reid MB (2000) Cardiac-specific overexpression of tumor necrosis factor- α causes oxidative stress and contractile dysfunction in mouse diaphragm. *Circulation* 102:1690–1696
- Lowe DA, Surek JT, Thomas DD, Thompson LV (2001) Electron paramagnetic resonance reveals age-related myosin structural changes in rat skeletal muscle fibers. *Am J Physiol (Cell)* 280:C540–C547
- Moisescu DG, Thieleczek R (1978) Calcium and strontium concentration changes within skinned muscle preparations following a change in the external bathing solution. *J Physiol* 275:241–262
- Muller FL, Song W, Liu Y, Chaudhuri A, Pieke-Dahl S, Strong R, Huang TT, Epstein CJ, Roberts LJ, Csete M, Faulkner JA, Van Remmen H (2006) Absence of CuZn superoxide dismutase leads to elevated oxidative stress and acceleration of age-dependent skeletal muscle atrophy. *Free Radic Biol Med* 40:1993–2004
- Panchangam A, Witte RS, Claffin DR, O'Donnell M, Faulkner JA (2006) A novel optical imaging system for investigating sarcomere dynamics in single skeletal muscle fibers. *Proceedings of the SPIE* 6088(1):608808–608811
- Plant DR, Lynch GS, Williams DA (2000) Hydrogen peroxide modulates Ca²⁺ -activation of single permeabilized fibres from fast- and slow-twitch skeletal muscles of rats. *J Muscle Res Cell Mot* 21:747–752
- Plant DR, Gregorevic P, Williams DA, Lynch GS (2001) Redox modulation of maximum force production of fast-and slow-twitch skeletal muscles of rats and mice. *J Appl Physiol* 90:832–838
- Podolin RA, Ford LE (1986) Influence of partial activation on force-velocity properties of frog skinned muscle fibers in millimolar magnesium ion. *J Gen Physiol* 87:607–631
- Prochniewicz E, Lowe DA, Spakowicz DJ, Higgins L, O'Connor K, Thompson LV, Ferrington DA, Thomas DD (2008) Functional, structural, and chemical changes in myosin associated with hydrogen peroxide treatment of skeletal muscle fibers. *Am J Physiol (Cell)* 294:C613–C626
- Reid MB (2001) Invited review: redox modulation of skeletal muscle contraction: what we know and what we don't. *J Appl Physiol* 90:724–731
- Reid MB, Khawli FA, Moody MR (1993) Reactive oxygen in skeletal muscle. III. Contractility of unfatigued muscle. *J Appl Physiol* 75:1081–1087
- Sakellariou GK, Pye D, Vasilaki A, Zibrik L, Palomero J, Kabayo T, McArdle F, Van Remmen H, Richardson A, Tidball JG, McArdle A, Jackson MJ (2011) Role of superoxide-nitric oxide interactions in the accelerated age-related loss of muscle mass in mice lacking Cu, Zn superoxide dismutase. *Aging Cell* 10:749–760
- Supinski GS, Callahan LA (2007) Free radical-mediated skeletal muscle dysfunction in inflammatory conditions. *J Appl Physiol* 102:2056–2063
- Supinski G, Stofan D, Callahan LA, Nethery D, Nosek TM, Dimarco A (1999) Peroxynitrite induces contractile dysfunction and lipid peroxidation in the diaphragm. *J Appl Physiol* 87:783–791
- Thompson LV (2009) Age-related muscle dysfunction. *Exp Gerontol* 44:106–111
- Vasilaki A, van der Meulen JH, Larkin L, Harrison DC, Pearson T, Van Remmen H, Richardson A, Brooks SV, Jackson MJ, McArdle A (2010) The age-related failure of adaptive responses to contractile activity in skeletal muscle is mimicked in young mice by deletion of Cu, Zn superoxide dismutase. *Aging Cell* 9:979–990
- Wolledge RC, Curtin NA, Homsher E (1985) Energetic aspects of muscle contraction. Academic Press, Orlando